TWENTY-SECOND INTERNATIONAL CONFERENCE ON COMPOSITE MATERIALS (ICCM22)

INFLUENCE OF TEXTILE ARCHITECTURE ON THE MECHANICAL PROPERTIES OF 3D WOVEN CARBON COMPOSITES

Monali Dahale[1], Geoffrey Neale[1], Cormac McGarrigle[2], John Kelly[1], Edward Archer[1], Eileen Harkin-Jones[1] and Alistair McIlhagger[1]

[1] Engineering Research Institute, Ulster University, Shore Road, Newtownabbey, BT37 0QB, UK
Email: m.dahale@ulster.ac.uk, www.ulster.ac.uk/research/institutes/engineering

[2]Centre for Engineering and Renewable Energy, Ulster University, Magee Campus, BT48 7JL, UK

Keywords: 3D woven layer-layer, pick density, float length, mechanical properties, micro-computed tomography

ABSTRACT

The application of 3D woven composites in advanced structural components is limited by a lack of understanding of the influence of weaving parameters on the final architecture and mechanical properties of composites. This paper investigates the effect of fundamental and easily adjustable weave parameters (pick density and float length) on the mechanical properties (tension, compression and flexure) in 3D woven warp interlock layer-to-layer carbon/epoxy composite structures. The purpose of this paper is to establish a link between the textile and composite performance within this 3D weave architecture. The 3D fabrics, manufactured using a Jacquard loom, are fabricated in three different pick densities: 4, 10 & 16 wefts/cm, with a constant end density of 12 warps/cm from T700S-50C-12k carbon fibre. The pick density with the best mechanical properties is then used for the float length change iteration. The aim is to keep end and pick densities constant in the two float length variation specimens. The mechanical properties of the specimens are affected by the fibre content, tow waviness, misalignment of the load carrying tows and the distribution/size of resin rich areas. This paper depicts a link between the pick density/float length, mechanical properties and failure mechanisms in 3D woven layer-to-layer carbon/epoxy composites.

1 INTRODUCTION

3D weaving is an interlacement of three yarns (warp, weft and binders) in three mutually perpendicular directions to manufacture textile preforms of considerable thickness [1]. Reinforcing fibres (binders) in the through-thickness direction in 3D woven composites eliminate delamination as a mode of failure [2][3] and substantially improves the composite damage tolerance and out-of-plane properties [4]. Moreover, 3D woven composites are starting to pick up traction in both aerospace and automotive industry due to their multi-directional load bearing capacity, low cost to performance ratio and capability to manufacture near-net-shaped preforms reducing the overall manufacturing cost [5]. However, the in-plane properties of 3D woven composites are generally compromised as compared to the fibre-reinforced composite laminates due to increased fibre crimping [6].

3D woven fabrics can be divided into three fundamental and most widely used weave architectures, orthogonal, layer-to-layer and angle interlock [7]. All three architectures are distinguished from one another by the positioning of binder yarns. In orthogonal and angle interlock architectures the binder yarn goes through the thickness whereas in layer-to-layer type architecture the binder yarn connects above and below the weft layers immediately. The weave architecture has a direct influence on the unit cell size, tow crimp and tow misalignment subsequently affecting the mechanical properties of 3D woven composites [8]. In the existing literature, the mechanical performance of angle interlock and orthogonal 3D woven architectures have been extensively studied while layer-to-layer being seldom explored. Although the orthogonal architecture has better through-thickness properties (higher V_f in the z direction) as compared to layer-to-layer and angle interlock architectures, it lacks its capability to provide high drapability around complex geometric structures [9]. The layer-to-layer architecture possesses high conformability and only one-sixth specific energy absorption (SEA) loss on the transition

from quasi-static to high-speed dynamic loading as compared to other architectures [10]. This less energy absorption loss on the transition from low to high strain rates is beneficial for crash applications in the automotive industry.

There is a lack of understanding of how the weave parameters and geometrical flaws like the misalignment, voids, resin rich areas and certain topological features of the weave architecture influence the mechanical properties and failure mechanisms in these materials. In the current literature, comparisons are made between three standard architectures (angle interlock, orthogonal & layer-to-layer) of 3D woven composites[11][7]. In order to establish a fair comparison and to develop an understanding of the relationship between the weave parameters in textiles and their influence on mechanical properties of composite materials, two easily adjustable weave iterations in 3D layer-to-layer architecture are considered for this study.

The purpose of this paper is to study the effect of pick density and binder float length on the mechanical properties of 3D woven layer-to-layer composites. The pick density and float length changes in 3D woven preforms can be achieved by slight changes in the manufacturing process. The pick density can be adjusted by changing the speed of the take-up whereas the float length change can be achieved by modifying the textile design plan. Both these parameters can be achieved without the need to rethread the entire loom, which is an exponentially time-consuming process (over 100 hours, varies with architecture, warp/binder density etc). Also, rethreading the entire loom can cause severe damage to the warp and binder yarns which ultimately knocks down the performance of the subsequent composite materials. The effect of pick density and float length in 3D woven layer-to-layer carbon composite has been studied on the in-plane properties (tension and compression) and out-of-plane properties (three-point bending test). The effects of the weave architecture on the physical properties of the composite, like its compaction, areal density, thickness and fibre volume fraction (v_f) are also examined. In-depth failure mechanism analysis under different loading is carried out using micro-computed tomography. Understanding the failure mechanisms helps to eliminate the microstructural features that degrade the performance of 3D woven composite structures.

2. MATERIALS

2.1 Manufacture of 3D woven textile preforms

A 3D woven layer-to-layer architecture was selected for this study due to its high drapability around complex geometric structures. Three different pick densities (4, 10 and 16 wefts/cm) and a constant warp density of 12 ends/cm in a layer-to-layer architecture were designed using ScotWeave software (Figure 1). These specimens are referred to as WD1, WD2 and WD3 for low, medium and high pick density respectively. The lift plan (Figure 1d) was developed at Ulster University using the same ScotWeave software to run DATAWEAVE controlled jacquard loom. The 3D woven preforms were manufactured by Axis Composites Ltd. The creel was set-up for 600 bobbins in order to weave 12 ends/cm for a 50 cm wide textile preform. A beat-up reed with 1dent/cm was used to space the warp yarns. The architecture consisted of three warp layers, four weft layers and three warp binder layers which connect weft layers immediately above and below each individual binder. In Figure 1, binder yarns are shown in red, stuffer yarns in blue and weft yarns are light green. T700S-50C-12k (800 Tex) [12] carbon fibre was used in the manufacture of all specimens in all three directions. Figure 2 shows the 3D woven preforms manufactured on the Jacquard loom in three pick densities.

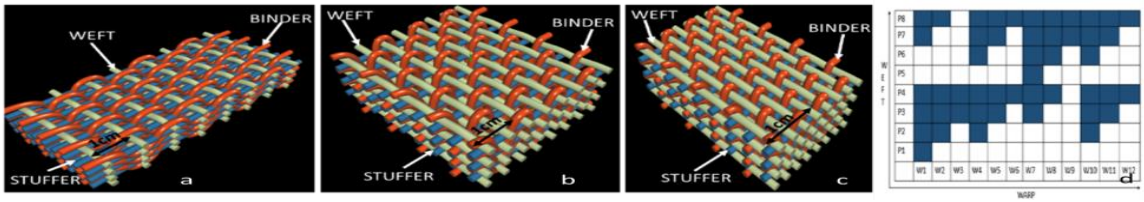

Figure 1: Diagrams representing (a, b, c) the 3D woven layer-to-layer architecture in three weft densities (4, 10, 16 wefts/cm) (d) Lift plan for Jacquard loom

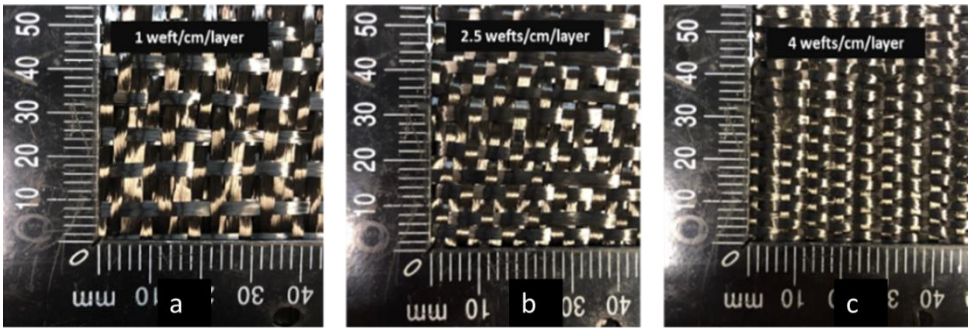

Figure 2: 3D woven carbon preforms (a) WD1 (b) WD2 and (c) WD3.

The pick density with superior mechanical performance was used to manufacture specimens with float length change iteration. The end density was kept constant in the float length change iteration. Lift plans for two different binder float length (1 & 3) were designed using ScotWeave design software. These specimens are referred to as FL1 and FL2 respectively. Figure 3 shows the architecture and woven preform of two different float lengths (FL1 and FL2) considered in this study.

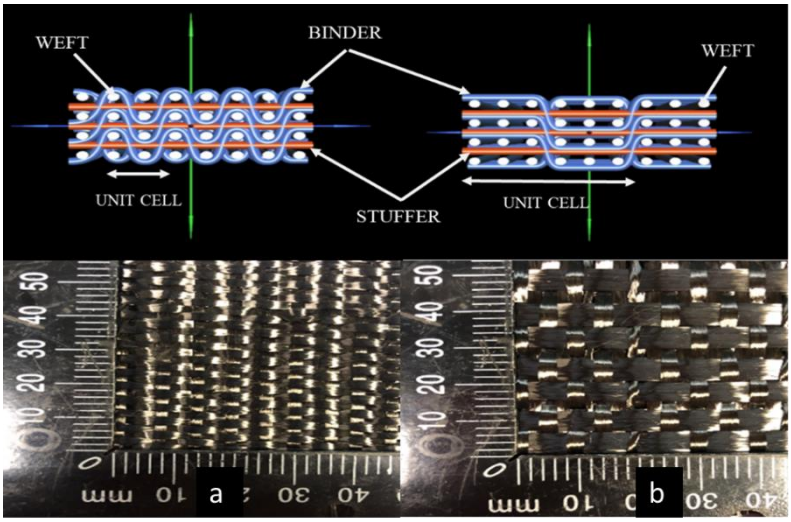

Figure 3: Architecture and 3D woven preforms of two float length change iteration (FL1 and FL2)

2.2 Manufacture of 3D Woven Composite

The textile preforms woven in pick density (WD1, WD2 & WD3) and float length (FL1 & FL2) iteration were consolidated via Resin Transfer Moulding (RTM) using a Gurit Prime 20LV epoxy resin system [13]. Resin and hardener were mixed in 100:26 by weight ratio and stirred for two minutes in order to ensure uniform mixing. Prior to infusion, the mixture was degassed in a homogeniser for 30 minutes and then injected into a preheated (30℃) RTM tool designed for the consolidation of 400x400 mm preforms. The injection pressure was maintained at 0.75 bar throughout the infusion. After injection, the part was cured at 50℃ for 16 hours at 1 bar pressure.

3. EXPERIMENTATION

3.1 3D woven preform properties

The physical properties of the textile preforms, such as the weft density (number of transverse yarns per cm of the fabric), warp density (number of longitudinal yarns per cm of the fabric) and thickness were measured according to ASTM standards [14]–[16] respectively. Crimp measurements were made in accordance with BS 2863:1984. Percentage crimp is the ratio of the difference between the yarn length and fabric length over fabric length. It is calculated using the following equation:

$$\%\text{Crimp} = \frac{L_{yarn} - L_{fabric}}{L_{fabric}} \quad (1)$$

The average float length (F) of the binder is calculated according to Ashenhurst [17] equation which is:

$$F = \frac{R}{t} \quad (2)$$

Where R is the warp repeat and t is number of warp intersections in the weave repeat.

3.2 Mechanical properties

Five specimens each in warp and weft directions were tested under tension in accordance with ASTM 3039 [18] using a Zwick Universal Testing System (UTS) with a 100kN load cell. A crosshead displacement of 2mm/min was used to perform these tests. An extensometer was used to record strains up to 0.6% after which it was detached to prevent it from damaging due to shock waves. Five specimens in each direction (warp and weft) were tested for compression in accordance with a Boeing modified ASTM D695 [19] using an electromechanical Instron 5500R UTS machine with 100kN load cell and anti-buckling fixture. The original test was modified by changing the specimen shape and reducing the gauge length to 4.8mm in order to avoid buckling of the test specimens. Three-point bending tests were performed on five specimens in each direction in order to obtain the flexural strength and the modulus. This test was performed in accordance to ASTM D7264 standard [20] on an electromechanical Instron 5500R UTS machine with a 100kN load cell. Five specimens with a span to thickness ratio of 32 were tested oriented in both the warp and weft directions at a crosshead displacement of 1mm/min.

3.5 Micro-computed tomography

A Brunker SkyScan 1275 automated micro-CT system was used to observe the microstructural damage to study the failure mechanisms.

4. RESULTS & DISCUSSION

4.1 Effect of pick density on the mechanical properties

Physical properties of preforms and composites for pick density variation (WD1, WD2 & WD3) iteration are listed in Table 1. The warp density is kept constant whereas the pick density is increased from 4 to 16 wefts/cm. With the increase in the pick density, the density of the final composite increases slightly by 9.8%.

Fabric	Wefts /cm	Warps /cm	t* (mm)	Yarn content (%)			% Tow crimp in uncompressed preform		$v_{f\,(\%)}$
				Warp	Weft	Binder	Warp	Weft	
WD1	4	12	2.6	37.5	25	37.5	5.5	1.8	32.7
WD2	10	12	3	27.2	45.5	27.2	3.7	1.4	40.8
WD3	16	12	4.2	21.4	57.2	21.4	2.8	1.3	53.7

**t is the thickness of the uncompressed preform.*

Table 1: Preform and composite properties of three pick density change specimens

Figure 4 shows the tensile properties and density of WD1, WD2 and WD3 specimens in both warp and weft directions. In the weft direction specimens, there is a 70% and 52% increase in the tensile strength and modulus respectively going from WD1 to WD2 and 21% and 39% increase in the strength

and modulus respectively with the transition from WD2 to WD3 (Figure 4). This increase is expected as the fibre content of the load carrying yarns is increased with pick density change from WD1 (4 wefts/cm) to WD3 (16 wefts/cm) specimens. The tensile property increase is significantly higher going from WD1 to WD2 as compared to the WD2 to WD3 transition, this is thought to be a result of a greater decrease in the crimp (22.2%) from WD1 to WD2 as compared to 7.2% reduced crimp from WD2 to WD3 (Table 1). WD1 specimens have 67% more resin rich regions than in WD2 specimens (Figure 5), whereas negligible resin rich areas are observed in WD3 specimens due to its more compact structure. The presence of numerous resin rich areas in WD1 specimens promotes clean fracture rather than fibre pull-out or fibre fracture.

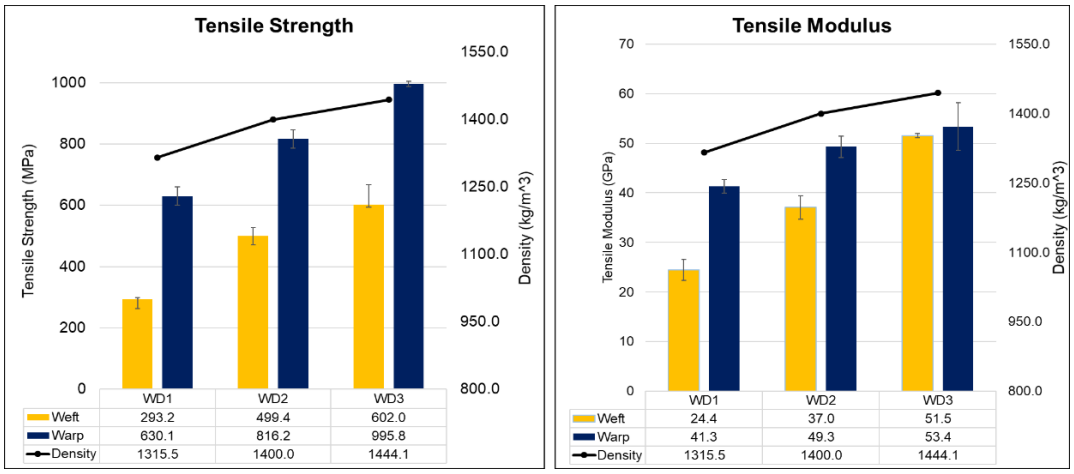

Figure 4: Tensile properties of three weft density specimens

The failure mechanisms transition (WD1 to WD2) from clear transverse matrix fracture, which is seen to be mostly uninterrupted by the weft yarns, to significant fibre pull out and fibre fracture in WD2 and WD3 specimens. In WD3 specimens, the primary crack is forced to propagate through the fibres and the increased number of fibres promote crack branching. More energy is required to break these fibres than is required to propagate through the matrix as observed in WD1.

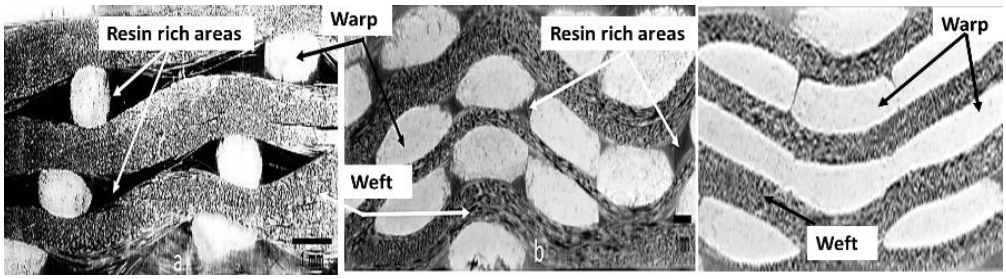

Figure 5: Micrographs of representative WD1, WD2 and WD3 specimens

From Figure 4 it is evident that the increase in pick density also significantly improves its performance in the warp direction. There is a 30% and 22% increase in the tensile strength and 19% and 8% increase in the tensile modulus with the transition from WD1 to WD2 and WD2 to WD3 respectively. This can be partially attributed to a decrease in crimp of 33% and 24% from the WD1 to WD2 and WD2 to WD3 transition respectively. The number of binding points per unit cell is highest in WD3 followed by WD2 and WD1. These binding points act as stress concentrations which result from resin rich regions around them. Warp direction failure transitions from being predominantly fibre-matrix debonding dominated (while fibres remain intact) to being dominated by fibre pull out and fibre fracture (Figure 6). In the WD1 specimens, the tow straightening event is so severe that the specimens do not cleanly fracture after ultimate strength is achieved (Figure 6a).

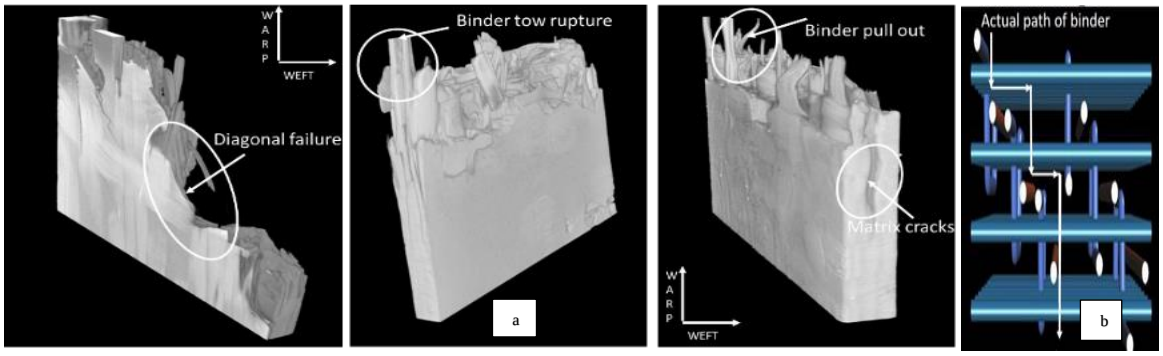

Figure 6:(a) Micro-CT images of failure in WD1, WD2 and WD3 specimens (warp direction); (b) WD1 architecture showing the path of crack propagation (Diagonal).

An interesting strain induced shear failure is observed in WD1 specimens (lowest weft density specimens) which was also reported by Dahale et al. [21] in 3D woven layer-to-layer glass/epoxy composites. The crack propagates through the thickness of the WD1 specimens and follows the path as shown in Figure 6b. This is a result of a more open architecture in the WD1 specimens which enables the binder yarns to become displaced from the original position instead of stacking neatly (Figure 5). The crack, after initiating in the resin rich areas, follows the binder position as shown in Figure 6b. This has resulted in a diagonal crack propagation through the thickness.

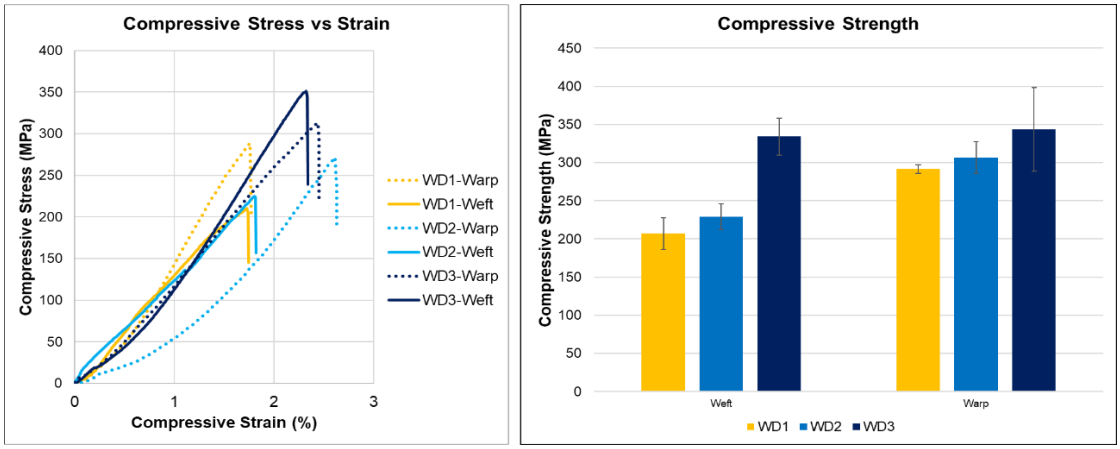

Figure 7: Compressive properties of three pick density specimens.

From Figure 7 it is evident that with increasing weft density there are significant improvements in the compressive strength in both warp and weft directions. In the weft direction, there is an increase of 11% and 46% compressive strength on the transition from WD1 to WD2 and WD2 to WD3 respectively. The increase in compressive strength in the weft direction is due to the significant increase in the percentage of fibres in that orientation.

There is a slight increase of 5% and 12% in strength on the transition from WD1 to WD2 and WD2 to WD3 respectively in the warp direction. This moderate increase in compressive strength is the direct result of higher geometric regularity in the composite in WD2 and WD3 specimens (Figure 5). As per the 3D woven preform design, WD3 specimens have a much smaller unit cell of 7 mm compared to WD1 specimen which is 16 mm. Smaller unit cell implies a greater number of binding points are compressed in the 4.8mm gauge length for compression testing compared to WD1 specimens. Due to increased binding points in WD3 specimens, more energy is required before the specimen fails. This leads to 19% increased compressive strength in WD3 compared to the WD1 specimens.

Architecture	Flexural Strength (MPa)				Flexural Modulus (GPa)			
	Warp	% COV*	Weft	% COV*	Warp	% COV*	Weft	% COV*
WD1	308.72	20.16	490.89	1.26	14.3	16.26	21.5	2.56
WD2	372.25	15.95	489.35	4.33	19.67	3.30	26.67	4.32
WD3	503.89	9.81	492.99	8.92	27.70	8.42	50.15	6.78

**COV is the coefficient of variation.*

Table 2: Flexural properties of three pick density change specimens (*Coefficient of variation).

*COV *is the coefficient of variation.*

Table 2 shows the flexural strength and modulus of three pick density specimens (WD1, WD2 & WD3). It is evident that with the increase in the pick density from WD1 to WD3, the flexural strength and modulus increases by 63% and 93% respectively in the warp direction. The compact structure in WD3 specimens compared to WD1 specimens makes it stiffer and more resistant against bending. Due to the tightly packed structure in WD3 specimens upon flexure loading, the primary crack is resisted by the closely spaced weft yarns. The crack initiates at the surface of the specimen and is resisted from going through the thickness (Figure 8c) whereas due to numerous resin rich areas and loosely packed structure enable in WD1 specimens, the crack propagates through the thickness of the specimen (Figure 8a). In the weft direction, the flexural strength remains the same with an increase in the pick density. This is a direct result of the constant end density of 12 warps/cm in all the three specimens (WD1, WD2 and WD3).

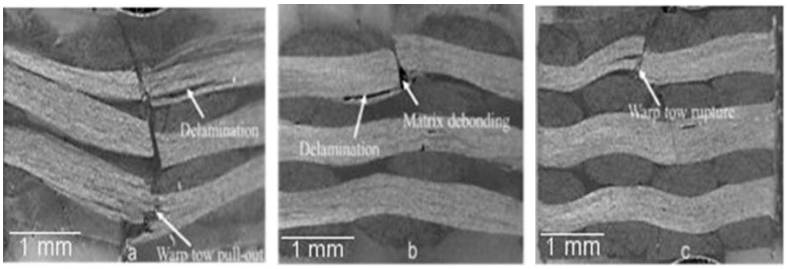

Figure 8: Micrographs of representative failed specimens in flexure for three pick densities (WD1, WD2 & WD3)

4.2 Effect of float length on the mechanical properties

Fabric Properties										Composite properties	
Fabric	Wefts/cm	Warps/cm	t* (mm)	F*	Yarn content (%)			%Tow Crimp		h* (mm)	V_f (%)
					Warp	Weft	Binder	Warp	Weft		
FL1	16	12	3.8	1	21.4	57.1	21.4	2.8	1.7	2.9	49.9
FL2	24	12	4.2	3	16.6	66.6	16.6	4.1	0.6	3.4	54.9

**t: thickness of uncompressed preform, *F: Average float length, *h: thickness of composite*

Table 3: Table showing variation in preform and composite properties of FL1 and FL2 specimens

Table 3 and Figure 9 shows the physical properties and micrographs of two float length change specimens (FL1 & FL2). The tow misalignment (Figure 9) and crimp (Table 3) are significantly higher in FL2 compared to the FL1 specimens. 53% numerous resin rich areas are observed in the micrographs of FL2 specimens compared to the FL1 specimens after analysis on ImageJ software (Figure 9). The numerous and larger resin rich areas in FL2 specimens are thought to be a result of distorted positioning of yarns in this architecture. In FL2 specimens (3 float), the two weft yarns sit next to each other but to maintain the pick density of 24 wefts/cm, the third weft yarn is pushed below, resulting in distortion of the warp binders and hence more resin rich areas.

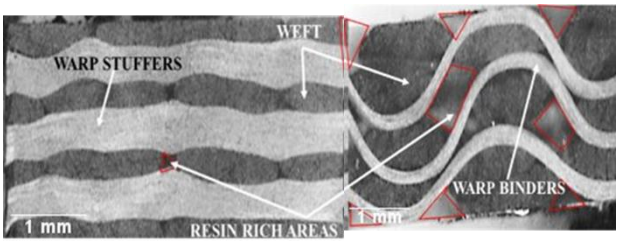

Figure 9: Micrographs of representative specimens of FL1 and FL2

From Table 4, it is evident that with the increase in the float length (FL1 to FL2), the tensile strength and modulus increases by 97% and 38% respectively in the weft direction. The aim of this float length study was to maintain the pick density constant for both FL1 and FL2 specimens. But in order to maintain the structural stability of the fabric [22] for this higher float (FL2) specimens the pick density was increased from 4 to 6 wefts/cm. It is also important to understand the manufacturing limitations (beat-up speed) on the jacquard loom to weave complex textile architectures. An increase in the tensile properties in the weft direction is a result of increased average float length from 1 to 3. This implies a greater proportion of three merged collimated weft yarns (increased % of in-plane weft yarns) which is also supported by 64% less crimp in FL2 specimens as compared to the FL1 specimens. Also, the percentage weft fibre content and pick density are increased by 17% and 50% respectively in the FL2 specimens in the weft direction. There is an increase of 32% in strain to failure on the transition from FL1 to FL2. This is possibly because maintaining the tension in the weft yarns for FL2 specimens during weaving is more difficult than for FL1 specimens due to slower weft insertion (as three wefts are inserted back-to-back in FL2 specimens). This leads to significant increase in the straightening of weft yarns in FL2 specimens before the specimens fail. This is supported by the failure modes observed in the weft direction for these specimens. The failure mode transitions from weft tow rupture to weft tow pull-out on going from FL1 to FL2. The weft pull-out is very significant in the FL2 specimens which implies higher load bearing capacity as compared to the FL1 specimens before the specimen failure [23] (Figure 10c & d).

Architecture	Property	Weft	Warp
FL1	Tensile Strength (MPa)	601.9	995.7
	Tensile Modulus (GPa)	51.5	53.3
	Strain to failure (%)	1.7	1.9
FL2	Tensile Strength (MPa)	1196.9	495.3
	Tensile Modulus (GPa)	71.2	36.7
	Strain to failure (%)	2.2	1.7

Table 4: Tensile properties of two float length change specimens

In the warp direction, with the increase in the float length, the tensile strength and modulus decrease by 50% and 32% respectively (Table 4). The overall percentage warp content decreases by 22% and the crimp in the warp tows increases by 46% on the transition from FL1 to FL2. The number of binder interlacement points are four times more in FL1 specimens due to a tightly packed unit cell.

This binding points act as stress concentration regions and increases the friction between the warp and weft yarns. At these binding points, the layer-to-layer interlaced binder yarns try to straigthen out upon tensile loading before the final fracture. Changing the float length from 1 (FL1) to 3 (FL2), decreases the binder fibre volume fraction content by 29% due to decrease in through-thickness components of binder yarns. This increases the weft yarns fiber volume fraction due to accommodation of more weft yarns under z-yarn float. The increase in weft yarn fibre volume fraction is more than the decrease in binder-yarn volume fraction and hence the total FVF increased with weave factor. This leads to a decrease in the tensile properties in the warp direction with the increase in the float length. Similar observations were made by Ozedimir et al. [24] in 2D woven composites, where they observed that with an increase in the average float length from 2.5 to 3 (3/1 twill to 4/1 twill), the tensile strength and modulus was decreased by 8% and 6% respectively in the warp direction. The significant tow misalingment in the warp direction of FL2 specimens leads to a 32% lower tensile modulus compared to FL1 specimens. A similar hypothesis was made by Quinn et al. [25] in 3D woven orthogonal composites, where they related the tow misalignment with the elastic modulus. The failure mode in the warp direction transitions from binder pull-out to binder tow rupture on the transition from FL1 to FL2 specimens (Figure 10a & b).

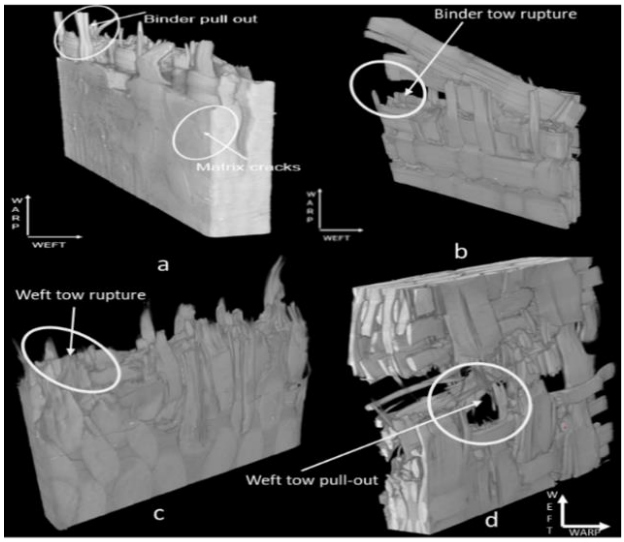

Figure 10: (a, b) Micro-CT images of representative FL1 and FL2 specimens in the warp direction; (c, d) Micro-CT images of representative FL1 and FL2 specimens in the weft direction

The compressive strength decreases by 46% on the transition from FL1 to FL2 in the warp direction (Figure 11). The gauge length for compression testing according to modified Boeing standard (ASTM D695) used for this study was 4.8mm. FL1 specimens have a unit cell of 7mm whereas FL2 specimens have a much larger unit cell of 16mm in the warp direction. It is impossible to fit an entire unit cell in the small gauge length proposed by this test. It is therefore very critical to produce good repeatability in the test results which led to a higher coefficient of variation in these specimens. Also, FL1 specimens have four times more binding points in a unit cell as compared to the FL2 specimens. This increases the amount of energy absorbed before the specimen fails to lead to higher compressive strength in the FL1 compared to the FL2 specimens in the warp direction.

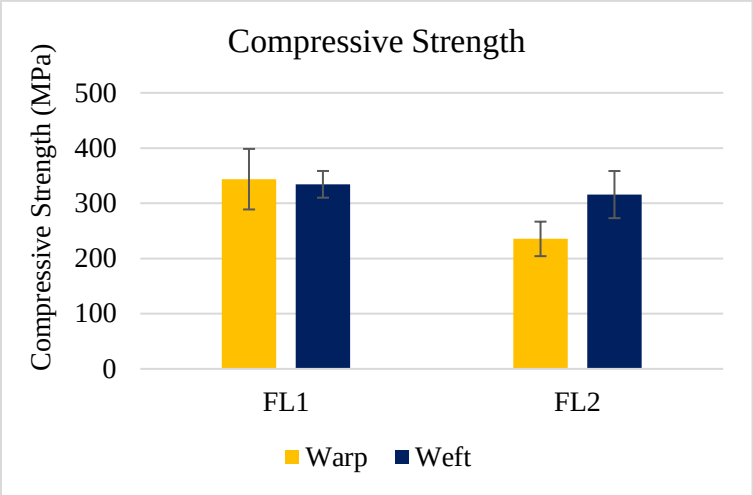

Figure 11: Compressive strength of two float length change specimens

Table 5 shows the flexural properties of two float length change specimens. On transition from FL1 to FL2, flexural strength and modulus increases by 66% and 34% respectively in the weft direction. Due to collimation of three weft yarns in FL2 specimens, the stiffness of these specimens increases and therefore it's resistance to bending. In the warp direction, the flexural strength and modulus decreases by 42% and 8% respectively. Cracks, initiating in the resin rich areas, goes through the thickness of the FL2 specimens whereas in the FL1 specimens (more compact structure) they are stopped by the next binder preventing the cracks from propagating through the thickness. This leads to longer delamination cracks and significantly more through thickness cracking in FL2 specimens compared to FL1 specimens (Figure 12). As seen in Figure 12, two warp tows are ruptured in FL2 specimens whereas in FL1 specimens the crack does not propagate through the thickness of the specimens. Significant matrix cracking is observed in FL2 compared to FL1 specimens due to numerous resin rich areas.

Architecture	Flexural Strength (MPa)		Flexural Modulus (GPa)	
	Warp	Weft	Warp	Weft
FL1	503.9	492.9	27.7	50.1
FL2	354.4	808.8	25.6	66.8

Table 5: Flexural properties of two float length change specimens (FL1 & FL2)

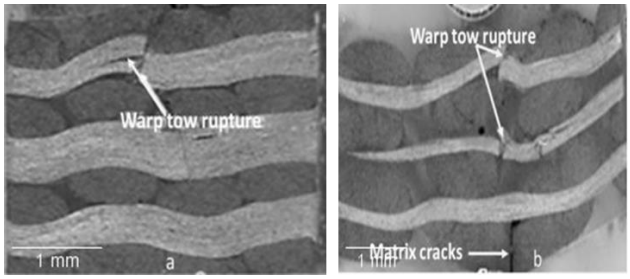

Figure 12: Micrographs of representative failed specimens in flexure (a) FL1 (b) FL2

5. CONCLUSION

The main objective of this paper was to study the influence of two weave parameters (pick density and float length) on the mechanical properties (tension, compression and flexure) of 3D woven warp interlock layer-to-layer carbon composites. The mechanical properties were improved in both the warp and weft directions with an increase in pick density (WD1 to WD3) that translates to a 9.8% density increase in the finished composite. The tensile strength was improved by 105% in the weft and 58% in the warp direction, compressive strength by 61% in the weft and 18% in the warp direction and flexural strength by 0.4% in the weft and 63% in the warp direction. It was found that changing the fibre content in the weft direction not only increases its mechanical properties in that direction but also significantly improves its performance in the warp direction (although the fibre content remains constant in the warp direction). This is thought to be result of a combination of several factors- V_f, tow misalignment, crimp, binding points/ unit cell and size/distribution of resin rich areas. With the increase in the float length, mechanical properties (tension, compression and flexure) were improved in the weft and deteriorated in the warp direction. The improvements in mechanical performance from WD1 to WD3 and FL1 to FL2 are achieved with a relatively small change in manufacturing parameters (increasing take-up speed and lift plan change) rather than a rethreading of the entire loom, which is an exponentially more time-consuming process.

ACKNOWLEDGEMENTS

This work is supported by EU Horizon 2020 Marie Skłodowska-Curie Actions Innovative Training Network- ICONIC [grant agreement number: 721256]. The authors acknowledge the support from The Engineering Research Centre (ECRE) of Ulster University and Axis Composites Ltd, especially Roy Brelsford, Dr Glenda Stewart, Simon Hodge and Graeme Craig.

REFERENCES

[1] N. Gokarneshan and R. Alagirusamy, “Weaving of 3D fabrics: A critical appreciation of the developments,” *Text. Prog.*, vol. 41, no. 1, pp. 1–58, 2009.

[2] J. Brandt, K. Drechslef, and F. Arendtsb, “Mechanical performance of composites based on various three-dimentional woven-fibre preforms,” *Compos. Sci. Technol.*, vol. 3538, no. 95, pp. 381–386, 1996.

[3] F. Chen and J. M. Hodgkinson, “Impact behaviour of composites with different fibre architecture,” *Proc. Inst. Mech. Eng. Part G J. Aerosp. Eng.*, vol. 223, no. 7, pp. 1009–1017, 2009.

[4] R. Gerlach, C. R. Siviour, J. Wiegand, and N. Petrinic, “In-plane and through-thickness properties , failure modes , damage and delamination in 3D woven carbon fibre composites subjected to impact loading,” *Compos. Sci. Technol.*, vol. 72, no. 3, pp. 397–411, 2012.

[5] P. Turner, T. Liu, and X. Zeng, “Collapse of 3D orthogonal woven carbon fibre composites under in-plane tension/compression and out-of-plane bending,” *Compos. Struct.*, vol. 142, pp. 286–297, May 2016.

[6] L. Tong A.P. Mouritz M. Bannister, *3D Fibre Reinforced Polymer Composites*. 2002.

[7] M. N. Saleh and C. Soutis, “Recent advancements in mechanical characterisation of 3D woven composites,” *Mech. Adv. Mater. Mod. Process.*, vol. 3, 2017.

[8] B. K. Behera and B. P. Dash, “Mechanical behavior of 3D woven composites,” *Mater. Des.*, vol. 67, pp. 261–271, 2015.

[9] M. Ansar, W. Xinwei, and Z. Chouwei, “Modeling strategies of 3D woven composites: A review,” *Compos. Struct.*, vol. 93, no. 8, pp. 1947–1963, 2011.

[10] J. Goering, H. Bayraktar, B. Stevenson, M. Mcclain, and D. Ehrlich, “Application of 3D Woven Composites for Energy Absorption,” *SPE Automot.*, pp. 1–18, 2015.

[11] R. Umer, H. Alhussein, J. Zhou, and W. Cantwell, *The mechanical properties of 3D woven*

composites. 2016.
[12] TORAYCA, "T700S TECHNICAL DATA SHEET CARBON," pp. 6–7.
[13] Gurit, "Prime ™ 20Lv Data Sheet." Gurit, pp. 1–6, 2015.
[14] ASTM International, "ASTM D3775 – 03a Standard Standard Test Method for Warp End Count and Filling Pick Count of Woven Fabric 1," vol. i, pp. 1–3, 2003.
[15] ASTM INTERNATIONAL, "D3775: Standard Test Method for Warp (End) and Filling (Pick) Count of Woven Fabrics," 2018.
[16] ASTM INTERNATIONAL, "D1777: Thickness of Textile Materials." 2015.
[17] K. H. Leong, B. Lee, I. Herszberg, and M. K. Bannister, "The e € ect of binder path on the tensile properties and failure of multilayer woven CFRP composites," vol. 60, pp. 149–156, 2000.
[18] ASTM International, "ASTM D3039/D3039M Standard test method for tensile properties of polymer matrix composite materials," *Annu. B. ASTM Stand.*, pp. 1–13, 2014.
[19] ASTM INTERNATIONAL, "D695: Compressive Properties of Rigid Plastics 1." 2015.
[20] ASTM International, "D7264/D7264M-15: Standard Test Method for Flexural Properties of Polymer Matrix Composite Materials," vol. i, pp. 1–11, 2015.
[21] M. Dahale *et al.*, "Effect of weave parameters on the mechanical properties of 3D woven glass composites," *Compos. Struct.*, vol. 223, p. 110947, May 2019.
[22] L. Thomas, *Woven structures and their impact on the function and performance of smart clothing*. Woodhead Publishing Limited.
[23] V. Giurgiutiu, K. L. Reifsnider, and C. A. Rogers, "Rate-independent energy dissipation mechanisms in fiber-matrix material systems A96-26890 AIAA-96-1420-CP," pp. 897–907, 1996.
[24] H. Özdemir, B. M. Içten, and A. Doğan, "Experimental investigation of the tensile and impact properties of twill and twill derivative woven fabric reinforced composites," *Tekst. ve Konfeksiyon*, vol. 28, no. 4, pp. 258–272, 2018.
[25] J. P. Quinn, A. T. McIlhagger, and R. McIlhagger, "Examination of the failure of 3D woven composites," *Compos. Part A Appl. Sci. Manuf.*, vol. 39, no. 2, pp. 273–283, Feb. 2008.